COMPUTER-AIDED MODELING OF THE RUBBER-PAD FORMING PROCESS

RAČUNALNIŠKO MODELIRANJE PREOBLIKOVALNEGA PROCESA Z VMESNIKOM IZ GUME

Muamar Benisa, Bojan Babic, Aleksandar Grbovic, Zoran Stefanovic

University of Belgrade, Faculty of Mechanical Engineering, Kraljice Marije 16, 11120 Belgrade, Serbia
bbabic@mas.bg.ac.rs

The conventional way to develop press-formed metallic components requires a burdensome trial-and-error process for setting-up the technology, whose success depends largely on the operator's skill and experience. The finite element (FE) simulations of a sheet-metal-forming process help a manufacturing engineer to design a forming process by shifting the costly press-shop try-outs to the computer-aided design environment. Numerical simulations of a manufacturing process, such as rubber-pad forming, have been introduced in order to avoid the trial-and-error procedure and shorten the development phases when tight times-to-market are demanded. The main aim of the investigation presented in this paper was to develop a numerical model that would be able to successfully simulate a rubber-pad forming process. The finite-element method was used for blank- and rubber-behavior predictions during the process. The study was concerned with a simulation and investigation of significant parameters (such as forming force and stress, and strain distribution in a blank) associated with the rubber-pad forming process and the capabilities of this process regarding the manufacturing of aircraft wing ribs. The simulation and investigation carried out identified the stress and strain distribution in a blank as well as the forming force. Experimental analyses of a rib with a lightening hole showed a good correlation between FE simulations and experimental results.

Keywords: rubber-pad forming, sheet-metal bending, finite-element simulation, aircraft manufacturing

Običajna pot pri razvoju stiskanih kovinskih komponent zahteva za postavitev tehnologije zamuden postopek z analiziranjem napak pri preizkusih, pri čemer je uspešnost odvisna od izvajalčeve spretnosti in izkušenj. Simulacija postopka preoblikovanja pločevine s stiskanjem po metodi končnih elementov (FEM) pomaga inženirjem pri postavljanju preoblikovalnega postopka z nadomeščanjem dragih preizkusov v računalniškem okolju. Da bi se izognili postopkom preizkušanja z analizo napak in ko je odločujoč kratek rok za trženje, so bile vpeljane numerične simulacije preoblikovalnega procesa, kot je preoblikovanje z vmesnikom iz gume. Glavni namen predstavljene preiskave je bil razvoj numeričnega modela, ki bi bil sposoben uspešne simulacije preoblikovalnega procesa z vmesnikom iz gume. Za napovedovanje dogajanj v stiskancu in v vmesniku iz gume je bila uporabljena metoda končnih elementov. Študija je obsegala simulacije in preiskave pomembnih parametrov (kot so preoblikovalna sila, napetosti ter razporeditev deformacije v preoblikovancu), povezanih s preoblikovanjem z vmesnikom iz gume in z zmogljivostmi tega procesa pri izdelavi reber letalskega krila. Izvršena simulacija in preiskava je odkrila napetosti in razporeditev deformacije v preoblikovancu, kot tudi sile pri preoblikovanju. Analiza reber z luknjo za zmanjšanje mase je pokazala dobro ujemanje med FE-simulacijo in eksperimentalnimi rezultati.

Ključne besede: preoblikovanje z vmesnikom iz gume, krivljenje pločevine, simulacija končnih elementov, izdelovanje letal

1 INTRODUCTION

Stamping is a metal-forming process, with which the sheet metal is punched using a press tool that is mounted on a machine or a stamping press forming the sheet into the desired shape. The conventional stamping process is performed through a punch, which, together with a blank holder, forces the sheet metal to slide into a die and comply with the shape of the die itself. Computers allow us to obtain and process data to improve and accelerate an analysis of the information required to optimize the processes of metal forming and to minimize the production costs.[1]

Rubber-pad forming is a metalworking process where sheet metal is pressed between a die and a rubber block. In general, an elastic upper die, usually made of rubber, is connected to a hydraulic press. A rigid lower die, often called a form block, provides the mold for the sheet metal to be formed. Because the upper (male) die can be used with different lower (female) dies, the process is relatively cheap and flexible. However, rubber pads exert less pressure in the same circumstances than the non-elastic parts, which may lead to a lower accuracy of the forming process. The form-block height is usually less than 100 mm.[2]

In the rubber-pad forming process an aluminum blank is placed between a die and a rubber pad (flexible punch), which is held in a container to enclose the flexible punch (**Figure 1a**). At this stage, the flexible punch (rubber-pad) is fixed on the arm of a pressing machine and the punch is on a machine table. As the rubber-pad moves down the rubber deforms elastically and offers a counter pressure. Due to this pressure the rubber-pad and the blank flow into the cavity of the die. This process can be divided into three steps: the first, self-forming of the rubber, the second, when the blank moves to the bottom of the die and produces the outer bending, and the third when the rubber pad pushes the blank into the cavity of the die.

In the aircraft industry most of the sheet parts, such as ribs, frames, doors and windows, are fabricated using
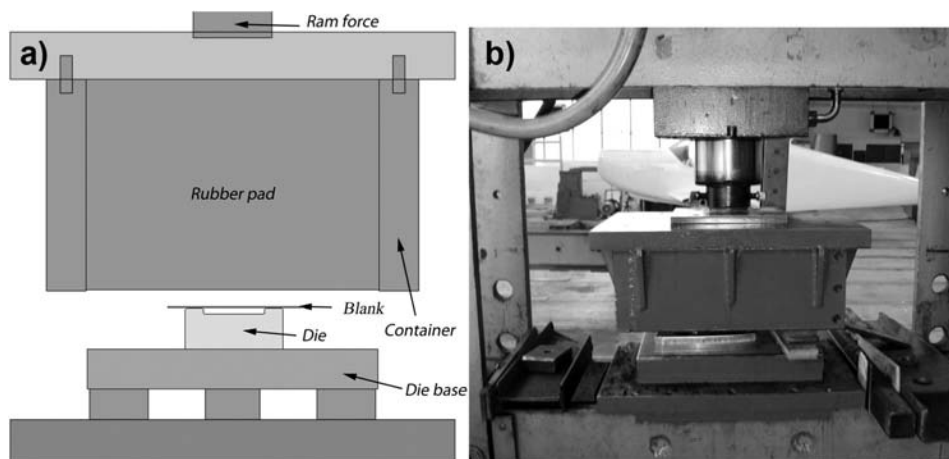
Figure 1: a) Schematic representation of a rubber-pad forming process, b) Experimental tool set-up
Slika 1: a) Shematski prikaz preoblikovalnega procesa z vmesnikom iz gume, b) eksperimentalno orodje

the rubber-pad forming processes (flexible tools). The advantages of using the rubber-pad forming process instead of the conventional metallic tools are: (i) the same flexible pad can be used to form several different work-piece shapes, because a rubber pad has the ability to return to its original shape; (ii) the tool costs are lower than the costs for the conventional forming processes; (iii) the thinning of the work metal, which occurs during the conventional deep drawing, is reduced considerably; (iv) the set-up time can be reduced considerably in this process, because no die clearance or alignment checks need to be made; (v) lubrication is not necessary and good surface finish can be achieved, because no tool marks are created. However, the rubber-pad forming processes have several disadvantages, such as: (i) the lifetime of a flexible pad is limited (this depends on the severity of forming combined with the pressure level); (ii) a lack of a sufficient forming pressure results in the parts with a lower sharpness or with wrinkles, which requires the reworking of the parts to their correct shape and dimensions; (iii) a low production rate, so that they are suitable mostly for small series (typical of the aircraft industry).[2–5]

Several studies have been carried out to analyze the rubber-pad forming. Browne and Battikha[6] presented an experimental study of the rubber-pad forming process to investigate the capability of the process and optimize the process parameters. Sala[3] optimized the rubber-pad forming of an aluminum-alloy fuselage frame belonging to an AerMacchi MB-339 trainer aircraft using his own finite-element code. Several effects have been investigated depending on stamping velocity, geometry, heat treatment of the sheet metal and rubber-pad parameters. Dirikolu and Akdemir[7] investigated the influence of rubber hardness and blank-material type on stress distribution using a 3D finite-element-simulation study of a flexible forming process. The investigation showed that the variation of pad thickness does not cause a big change in the forming stress in a blank. Madoliat and

Narimani[8] presented sheet forming by using a rubber pad and also investigated, experimentally and numerically, the design for the tooling set. Thiruvarudchelvan,[9] presented in this overview, highlighted the role of urethanes that are considered to be the best materials for flexible tools because of their good oil and solvent resistance, good wear resistance, high thermal stability and load-bearing capacity. Ramezani and Ahmed[5] carried out a numerical simulation of a rubber-pad forming process, along with an experimental validation, using a die of a flexible punch. They studied some forming parameters such as rubber type, stamping velocity, etc., and found that silicone rubber has a shorter lifetime than polyurethane and natural rubber. As a result, it cannot be used to form blanks with sharp edges. No significant change in the blank thinning was discovered for 5 different stamping velocities. Lee et al.[10] have investigated the deformation characteristic using the rubber-pad bending of a structural aluminum tube. A 3D finite-element analysis was used to examine the effect of process parameters on deformation characteristics of an extruded aluminum tube, and the influence of the formable radius of a tube curvature on bending resistance. The relation between the bent profile of a material and the roller stroke was defined. Fabrizio and Loreddana[11] studied flexible forming of thin sheets from aluminum alloys using different geometries and materials for the flexible die. They have investigated the forming force during a forming process for different dies.

These investigations showed that a numerical model can help us better understand the forming procedure, and the correlations with experimental results were good. M.W. Fu and H. Li[12] have presented 3D-FE simulations and investigated the deformation behavior of the flexible-die-forming process. The comparison between the conventional deep drawing and a viscoplastic carrying medium based on flexible-die forming was conducted in terms of wall-thickness reduction, hydro-

static pressure, principle-stress distribution and damage factor. The concave and convex rubber-pad forming processes were investigated by Liu, et al.,[13] using FE simulations and experimental methods. The investigations of the forming load, thickness variation of the formed plate and variations in the channel-width-to-rib-width ratio were also performed. A fabrication of a metallic bipolar plate for a proton membrane in fuel cells is presented in[14]. The FE analyses were used to describe the rubber-pad forming process and to investigate the main parameters (such as rubber hardness and dimensions of the rigid die). It was found that the smaller the internal radius, the harder it is to fill the cavity of a rigid die. The authors examined whether the blank filled the cavity of the rigid die by using a 3D-laser-scanning measurement system.

In this paper, numerical simulations of rubber-pad forming processes are used to analyze the blank and the rubber behaviors during a production of supporting ribs, as well as to analyze different punch geometries. A non-linear FE analysis was conducted to predict stress and strain distributions, and forming forces during the rubber-pad forming process. The main goal was to develop a computer model that would be able to simulate the process and, therefore, to develop the right design for a tooling set.

2 FINITE-ELEMENT MODELING AND EXPERIMENTAL VERIFICATION

Numerical simulations of the rubber-pad forming processes are complicated mainly because of a large deformation of a rubber pad. As a consequence, a mesh distortion may occur in a simulation, which can lead to inaccurate and incomplete results. This is why FE analyses must be carried out carefully and with an understanding of the physical phenomena of the rubber-pad forming process.

The commercial finite-element software Ansys® was used to make an FE simulation in this study. In order to reduce the processing time and improve the precision of the calculations, 2D FE models were created for three different sheet-metal elements (straight rib, stringer and rib with a lightening hole) and analyses were carried out for each model. **Figure 2** illustrates these three geometrical models. The models in FE analyses included three elements only: a rigid die, a blank and a rubber pad (flexible punch). In order to simplify the numerical model, the container of the rubber pad was not modeled. To eliminate the influence of the container, the frictionless support constraints were applied on the opposite sides of the rubber, while a displacement constraint was applied on the upper edge of the 2D rubber model (**Figure 3**).

The die was modeled as a rigid body because the stress and strain of the die were not analyzed and the die material (steel) is much less deformable than the material
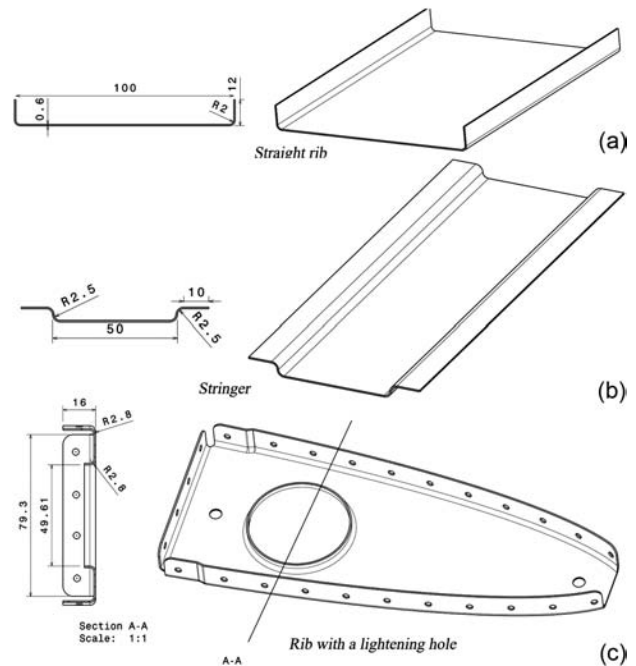

Figure 2: Geometrical models used in the investigation: a) straight rib, b) stringer and c) rib with a lightening hole
Slika 2: Geometrijski modeli, uporabljeni pri preizkušanju: a) ravno rebro, b) rebrasto rebro in c) rebro z luknjo za zmanjšanje mase

of the blank (aluminum). So, the material properties attached to the die were not important, and the mesh was not generated either. This eliminated unnecessary calculations causing a decrease in both the run time and the errors in the numerical solution.

Because the blank undergoes a large plastic-strain deformation during the forming process, the stress-strain test data up to a failure was required to define the blank material in the simulation (**Figure 4**). The blank was considered as a multilinear isotropic hardening material. In the FE simulations of the blank behavior, the von Mises yield criterion coupled with an isotropic work-hardening assumption[15] was used.

The rubber pad undergoes a nonlinear hyper-elastic deformation. The behavior of the nonlinear hyper-elastic and incompressible rubber-like material is usually described with the Mooney-Rivlin model that uses a strain-energy function W. The derivative of W, with
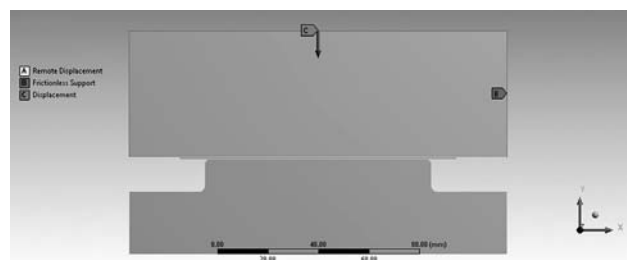
Figure 3: Constraints used in the FE simulation
Slika 3: Omejitve, uporabljene pri FE-simulaciji
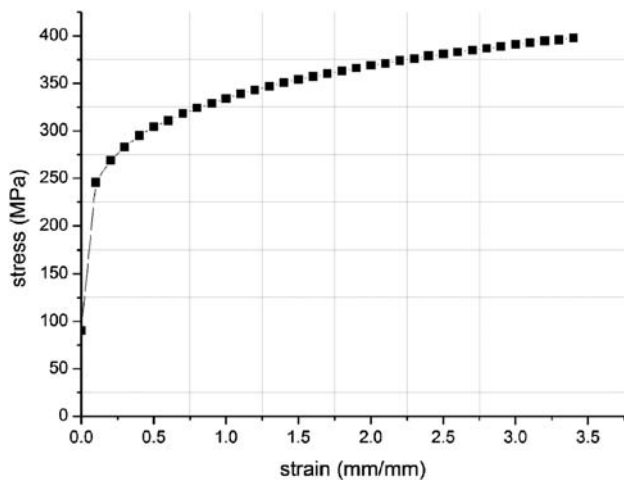
Figure 4: Experimental tensile-stress-strain curve for the aluminum blank sheet
Slika 4: Eksperimentalna krivulja napetost – raztezek za aluminijevo pločevino

respect to the strain component, determines the corresponding stress component:

$$\sigma_{ij} = \frac{\partial W}{\partial \sigma_{ij}} \qquad (1)$$

$$W = \sum_{k+m+1}^{n} C_{km}(I_1 - 3)^k + (I_2 - 3)^m + \frac{1}{2} k(I_3 - 1)^2 \qquad (2)$$

where I_1, I_2 and I_3 ($I_3 = 1$) are the strain invariants, k is the bulk modulus and C_{km} is the constant of the Mooney-Riviin material model for the incompressible material. Usually, two Mooney-Rivilin parameters, C_{10} and C_{01}, are used to describe the hyper-elastic rubber deformation.[7] In the FE models, the polyurethane rubber with the Shore A hardness of 70 (HD70) was used for the rubber pad. The values of C_{10} and C_{01} were 0.736 MPa and 0.184 MPa, respectively.[5,7,13,14]

An aluminum plate with a thickness of 0.6 mm was used as the blank. The aluminum properties were determined via the stress-stain curve obtained from the tensile tests,[7,16] as shown in **Figure 5**. For this alloy, the elastic module (E) is 71G Pa and the Poisson's ratio (ν) is 0.334.

During the rubber-pad forming process, the materials exhibit large deformations and rotations. There is a friction contact at the blank interfaces, too. At the same time, geometric nonlinearities arise from a nonlinear strain-displacement relationship, as well as the nonlinearities associated with the material properties. According to that, the geometric nonlinearity option was activated in the nonlinear solution procedure.

The friction behavior between the two different pairs of contact (rubber pad–blank and blank–die) was assumed to follow the Coulomb's model.[5,7] The friction coefficients for the former and latter contact pairs were considered to be 0.2 and 0.1, respectively.[5,7,13] **Table 1** shows the specifications of the contact region.

The interface contacts of the blank–rubber pad, blank–die and die–rubber were modeled as deformable and the software used solves these tasks on the basis of the contact-target-surface approach with an adjustable impenetrability constraint that assures contact compatibility. The CONTA 175 (a node-to-surface contact) finite element was used on the blank's surfaces at the interface between the blank and the die and on the rubber surface at the interface between the rubber and the die. The CONTA171 (a surface-to-surface contact) was used on the surface of the rubber pad at the interface between the blank and the rubber pad. The other surfaces at each interface were modeled with the TARGE169 element. It can be summarized that, in all the interface contacts, the upper surfaces of the die and the blank were considered as a target, while the lower surface of the blank and the upper surface of the rubber pad were considered as a contact.[17]

As mentioned above, the container was not modeled, so – in order to fix the rubber pad correctly – frictionless supports had to be applied on the side edges of the rubber. A remote displacement was applied on the lower edge of the die. A displacement was applied on the top edge of the rubber in order to simulate a forming load on the blank (**Figure 3**). All deformable materials were modeled with a Plane-183 finite element (a 2-D element with 8 or 6 nodes). Plane 183 has quadratic displacement, plasticity, hyper-elasticity, creep, stress stiffening, large deflection and large strain-simulation capabilities. The number of nodes and elements used for the blank and the rubber pad are presented in **Table 2**.

**Table 1:** Interface contacts
Tabela 1: Vmesni stiki

Parts in the contact	Contact type
Die & Blank	Frictional contact (0.1) node to surface
Blank & Rubber	Frictional contact (0.2) surface to surface
Die & Rubber	Frictional contact (0.1) node to surface

Table 2: Numbers of the nodes and elements for three models
Tabela 2: Število vozlov in elementov za tri modele

Modes	Blank		Rubber pad		Rigid die	
	Nodes	Element	Nodes	Element	Nodes	Element
Straight rib	2161	1680	4253	3958	205	204
Stringer	768	157	7254	2299	304	152
Rib with a lightening hole	863	615	5490	5181	208	207

In order to validate the FE simulations results, the rubber-pad forming experiments were carried out for the stamping of an aluminum blank. An experimental set-up (shown in **Figure 1b**) was used, together with the assembly of a die set shown in **Figure 1a**. The die and the rubber-pad container were made of steel, while polyurethane rubber with a Shore A hardness of 70 (HD70) was used as a rubber pad. A hydraulic press machine (produced by REXROTH), with the maximum
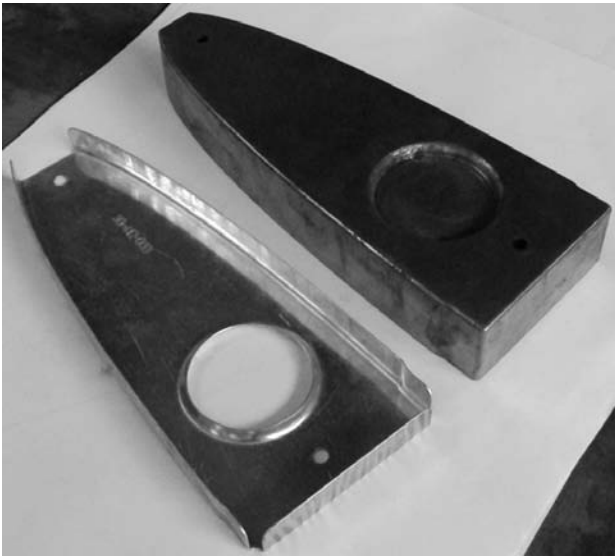
Figure 5: Rib with a lightening hole fabricated by the rubber-pad forming process and the die

Slika 5: Rebro z luknjo za zmanjšanje mase, izdelano z vmesnikom iz gume in orodje

capacity of 160 t was used in the rubber-pad forming process. The process begins with the die placed on the base of the hydraulic press machine. The aluminum blank is then introduced between the die and the flexible punch. After this the flexible punch moves down to stamp the blank. One of the formed parts fabricated during the rubber-pad forming process and the die used during the fabrication are shown in **Figure 5**.

3 RESULTS AND DISCUSSION

In this study, as mentioned above, the forming force was presented as a displacement applied on the upper edge of the rubber pad. **Figure 6** illustrates the step-by-step forming process using the rubber pad. It is clear that the process can be divided into three stages (or steps). The first stage is a self-deformation of the flexible die (the rubber pad); the second stage includes a blank deformation (under the pressure of the rubber pad when it reaches the bottom of the rigid die); and, finally, during the third stage the blank fills the die cavities until they are completely filled.

The convergences of the forming forces for each model, obtained through the FE simulations, are shown in **Figure 7**. This figure shows that the highest value of a forming force is present in the rib with a lightening hole (6735 N), while the lowest value is achieved in the straight rib (867 N). It can be seen that the magnitude of a forming force increases as the geometry of a rib becomes more complex, i.e., as more bending regions have to be obtained (**Table 3**).

The FE simulation of the forming process for the stringer and the rib with a lightening hole goes through three stages/steps (corresponding to the forming process), while the straight-rib forming can be performed in the first two steps (because there is no cavity to fill). During the first step – the self-forming of the rubber – the rubber deforms elastically and offers a counter pressure, so the forming load is very small (**Figure 6**). The time needed for this step is short (between 0.2 s and 0.35 s in the simulation – **Figure 7**). After 0.2 second (the straight rib) and 0.35 second (the other models), the second step starts and the forming load increases slightly to produce the outer bending (**Figure 5**). During the last step, after approximately 0.65 second, the blank starts to fill the cavity of the rigid die and the forming force increases sharply (**Figures 6** and **7**). According to the results of the FE simulations, it is obvious that the highest value of the forming force will be obtained in the
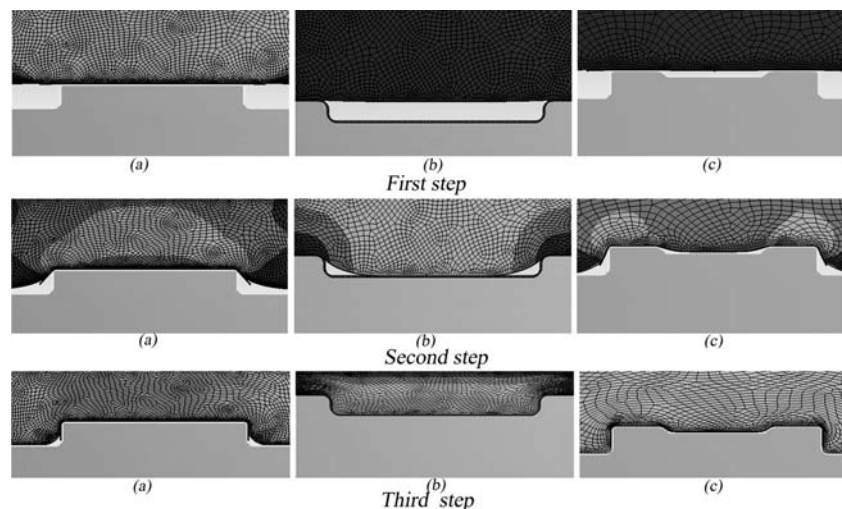
Figure 6: Forming steps during the rubber-pad forming including the first, the second and the third steps: a) straight rib, b) stringer and c) rib with a lightening hole

Slika 6: Stopnje med preoblikovanjem z gumijastim vmesnikom, vključno s prvo, drugo in tretjo stopnjo: a) ravno rebro, b) rebrasto rebro, c) rebro z luknjo za zmanjšanje mase
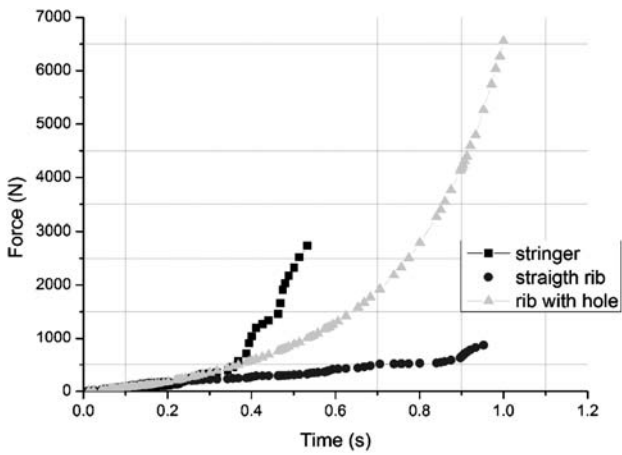
Figure 7: Forming force in three models
Slika 7: Preoblikovalna sila pri treh modelih

case of the most complex sheet-metal geometry (the rib with a lightening hole), where several bends with different radii must be produced. This is in correlation with the empirical data[3,7,13,14], which means that the used FE models have been well defined.

Along with the calculation of the forming force, stress and strain analyses were performed. As was expected, the stress and strain concentrations in a blank accumulate in the last two stages. **Figure 8** shows the equivalent stresses (in MPa, left column) and plastic strains (in mm/mm, right column) in the blanks at the end of the forming processes for all FE models. The summarization of the maximum and minimum stress and strain values, presented in **Figure 8**, is given in **Table 3**. **Table 3** shows that the maximum equivalent stress and plastic strain appear in the rib with a lightening hole (241.45 MPa and 0.206 mm/mm, respectively), while the minimum values of the equivalent stress and plastic strain are in the straight rib (224.74 MPa and 0.115 mm/mm, respectively). As can be seen in Table 3, the stress and plastic strain increase with an increased complexity of the rib geometry, as well as with an increased number of bend radii. The reason for that, according to Sala[3], is that the blank is exposed not only to the tensile and tangential stresses, but also to the stress arising from the bending pressure imposed by the tool. Consequently, the thinning phenomenon occurs homogeneously and, finally, the necking appears. The necking can induce a crack, which is not unusual in this forming process[5]. The crack starts when the blank undergoes stretching forces and when the ultimate stress is reached during the second or third stage of the forming process.

According to Sala[3] and Takuda[15], the maximum plastic strain that can be considered for the forming of this type of aluminum alloy is approximately 0.186 mm/mm. This value of plastic strain was used as a reference for the crack-appearance predictions in the FE simulations presented in this paper. The value of the plastic strain obtained in the forming simulation of the rib with a lightening hole (0.206 mm/mm) indicated the possibility of a crack appearance in the outer radius of the lightening hole, while the plastic-strain values for the other two models were less than 0.186 mm/mm.
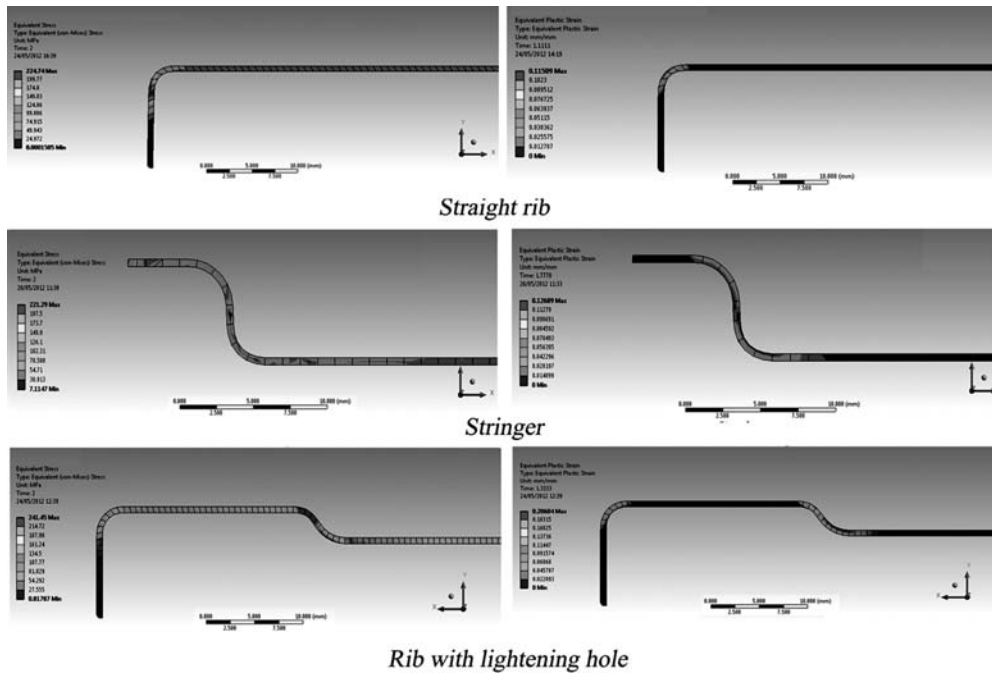

Figure 8: Equivalent stress (left column) and plastic strain (right column) in the straight rib, the stringer and the rib with a lightening hole (from the top)
Slika 8: Ekvivalentna napetost (leva kolona) in plastična deformacija (desna kolona) v ravnem rebru, rebrastem rebru in rebru z luknjo za zmanjšanje mase (od zgoraj navzdol)

Table 3: Summarization of the engineering requirements for the rubber-pad sheet-metal forming process
Tabela 3: Povzetek inženirskih zahtev pri preoblikovalnem procesu z vmesnikom iz gume

MODEL	Model 1 (straight rib)	Equivalent stress (MPa)	Equivalent plastic strain (mm/mm)	Reaction force N
Model 1 Straight rib	Maximum	224.74 (occurs on the blank)	0.115 (occurs on the blank)	866.43
	Minimum	1.2e-4	0.0	
Model 2 Stringer	Maximum	221.29 (occurs on the blank)	0.1268 (occurs on the blank)	2 734.7
	Minimum	7.032	0.0	
Model 3 Rib with a lightening hole	Maximum	241.45 (occurs on the blank)	0.206 (occurs on the blank)	6 553.8
	Minimum	0.101	0.0	
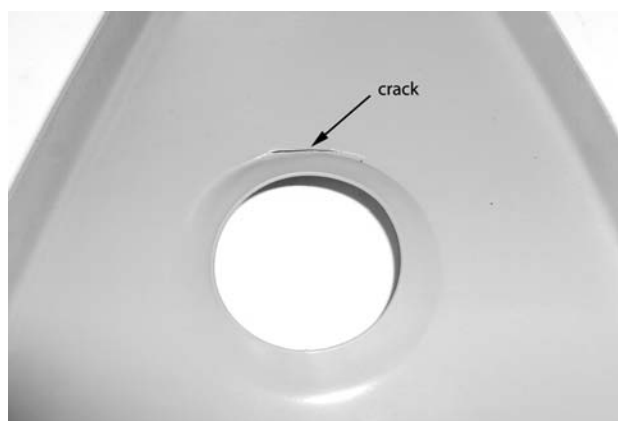
Figure 9: Rib with a crack around the lightening hole
Slika 9: Rebro z razpoko okrog luknje za zmanjšanje mase

The experiments with the rubber pad showed that the FE predictions were good. **Figure 9** shows the crack that appeared in the region around the rib hole during the third stage of the forming process, as predicted by the FE simulation. This was the proof of the quality of the developed finite-element model, as well as of the criterion proposed for this alloy (with the maximum plastic strain not exceeding 0.186 mm/mm). On the basis of these findings, more FE models of a rib with a lightening hole (with different values of the fillet radii) were developed and analyzed in order to find the connections between the values of a fillet radius and a plastic strain. These simulations showed that the values of stress and strain strongly depended on the rib geometry (i.e., the values of the fillet radii), but more investigations need to be performed in order to clearly define these dependencies.

4 CONCLUSION

A finite-element simulation of the rubber-pad forming process could be a very useful tool for understanding and improving the forming operations because it provides important data for determining the forming parameters and the operation time. The developed FE models and the method proposed in this paper have proved to be sufficiently effective in predicting the final shape of the component and the regions of a possible crack appearance.

The FE simulations showed that the maximum stresses and strains in all the cases were at the flanges and the corners. The minimum stress and plastic strain were achieved in the straight rib (the rib with the simplest geometry), while the maximum stress and plastic strain were found in the rib with a lightening hole (the most complex geometry). These results have been validated with the experiments, as well as with the fracture criterion used for the crack predictions. The FE simulations proved that simpler tools would reduce the lead times and enable a rapid production of small parts without a possibility of a crack appearance during the forming. On the other hand, the geometry of more complicated, but necessary, tools must be defined very carefully, with a determination of the fillet radii that will minimize the chance of a fracture. FEM can help us with this determination, too, while additional potential applications – such as 3D model simulations and tool optimization – are also possible.

However, it must be noticed that the optimization procedure of the press-forming processes – owing to the presence of the hardly reproducible phenomena like friction and lubrication – should never be limited to simple numerical simulations because the above phenomena can contribute a lot towards saving the costs and reducing the time-to-market, currently held up by empirical trial-and-error processes.

Sheet-metal-forming-simulation results, today, are reliable and accurate enough so that even the try-out tools and the time-consuming try-out processes may be eliminated, or at least reduced significantly.

5 REFERENCES

[1] A. Shramko, I. Mamuzic, V. Danchenko, The application of the program QFORM 2D in the stamping of wheels for railway vehicles, Mater. Tehnol., 43 (**2009**) 4, 207–211

[2] ASM Handbook Vol. 14B Metal Working: Sheet Forming, 2006

[3] G. Sala, A numerical and experimental approach to optimize sheet stamping technologies: part II – aluminium alloys rubber-forming, Material and Design, 22 (**2001**) 4, 299–315

[4] E. L. Deladi, Static friction rubber metal contact with application to rubber pad forming process, PhD Thesis, University of Twente, 2006

[5] M. Ramezani, Z. M. Ripin, R. Ahmad, Sheet metal forming with the aid flexible punch, numerical approach and experimental validation, CIRP Journal of Manufacturing Science and Technology, 3 (**2010**) 3, 196–203

[6] D. J. Browne, E. Battikha, Optimization of aluminium sheet forming using a flexible die, Journal of Materials Processing Technology, 55 (**1995**) 3/4, 218–223

[7] M. H. Dirikolu, E. Akdemir, Computer aided modelling of flexible forming process, Journal of Materials Processing Technology, 148 (**2004**) 3, 376–381

[8] R. Madoliat, R. Narimani, H. Rahrovan, Investigation of sheet metal forming using rubber pad forming, The SMEIR 2005 International Conference in Manufacturing Engineering, 2005, 1–9

[9] S. Thiruvarudchelvan, The potential role of flexible tools in metal forming, Journal of Materials Processing Technology, 122 (**2002**) 2/3, 293–300

[10] J. W. Lee, H. C. Kwon, M. H. Rhee, Y. T. Im, Determination of forming limit of a structural aluminum tube in rubber pad bending, Journal of Materials Processing Technology, 140 (**2003**) 1–3, 487–493

[11] F. Quadrini, L. Santo, E. A. Squeo, Flexible forming of thin aluminum alloy sheets, International Journal of Modern Manufacturing Technologies, 2 (**2010**) 1, 79–84

[12] M. W. Fu, H. Li, J. Lu, S. Q. Lu, Numerical study on the deformation behaviors of the flexible die forming by using viscoplastic pressure-carrying medium, Computational Materials Science, 46 (**2009**) 4, 1058–1068

[13] Y. Liu, L. Hua, J. Lanm, X. Wei, Studies of the deformation styles of the rubber-pad forming process used for manufacturing metallic bipolar plates, Journal of Power Sources, 195 (**2010**) 24, 8177–8184

[14] Y. Liu, L. Hua, Fabrication of metallic bipolar plate for proton exchange membrane fuel cells by rubber pad forming, Journal of Power Sources, 195 (**2010**) 11, 3529–3535

[15] H. Takuda, N. Hatta, Numerical Analysis of formability of an Aluminum 2024 alloy sheet and Its Laminates with Steel Sheets, Metallurgical and Material Transactions A, 29 (**1998**) 11, 2829–2834

[16] W. Eichlseder, Enhanced fatigue analysis – incorporating down-stream manufacturing processes, Mater. Tehnol., 44 (**2010**) 4, 185–192

[17] H. H. Lee, Finite Element Simulation with ANSYS Workbench12, Schroff Development Corporation, Taiwan, 2010